FULL PAPER

Soluble Flavanthrone Derivatives: Synthesis, Characterization and Application to Organic Light Emitting Diodes

Kamil Kotwica,[a] Piotr Bujak,*[a] Przemyslaw Data,[b,c] Wojciech Krzywiec,[a] Damian Wamil,[a] Piotr A. Gunka,[a] Lukasz Skorka,[a] Tomasz Jaroch,[d] Robert Nowakowski,[d] Adam Pron[a] and Andrew Monkman*[b]

Abstract: It is demonstrated that simple modification of benzo[*h*]benz[5,6]acridino[2,1,9,8-*klmna*]acridine-8,16-dione, an old and almost forgotten vat dye, involving reduction of carbonyl groups followed by O-alkylation, yields solution processable, electroactive, conjugated molecules of the periazaacene-type, suitable for the use in organic electronics. Their electrochemically determined ionization potential (IP) and electron affinity EA (*ca.* 5.2 eV and -3.2 eV) are essentially independent of the length of the alkoxy substituent and in good agreement with the DFT calculations. A crystal structure of 8,16-dioktyloxy-benzo[*h*]benz[5,6]acridino[2,1,9,8-*klmna*]acridine (**FC-8**), the most promising compound was resolved. It crystallizes in the $P\bar{1}$ space group forming π-stacked columns held together in the 3D structure by dispersion forces, mainly between interdigitated alkyl chains. **FC-8** molecules have a strong tendency to self-organize in monolayers deposited on a HOPG surface as observed by scanning tunnelling microscopy (STM). 8,16-Dialkoxy-benzo[*h*]benz[5,6]acridino[2,1,9,8-*klmna*]acridines are highly luminescent having photoluminescence quantum yields of *ca.* 80% in all cases. They yield efficient electroluminescence, and can be used as guest molecules with 4,4'-bis(*N*-carbazolyl)-1,1'-biphenyl (CBP) host in guest/host-type OLEDs. The best fabricated diodes showed luminance of *ca.* 1900 cd/m^2, luminance efficiency of *ca.* 3 cd/A and external quantum efficiencies (EQEs) exceeding 0.9%.

Introduction

Organic semiconductors of the acenes and azaacene families have been the subject of intensive research interest mainly due to their good electrical transport properties which make them interesting materials for applications in field effect transistors and other organic electronic devices.[1] Simple acenes and their derivatives such as rubrene (5,6,11,12-tetraphenyltetracene) or picene (dibenzo[*a,i*]phenanthrene), for example, exhibit very high values of charge carrier mobilities as compared to other p-type organic semiconductors.[2] Thus, acenenes are good p-type semiconductors, although their limited stability towards oxidative degradation should be noted. However, their reduction potential is very low and, as a result, their anion radical forms are extremely unstable. This excludes the use of acenes as potential n-type semiconductors or ambipolar field effect transistors (FETs).[1a,3]

Introduction of nitrogen atoms into the fused aromatic structure of acenes drastically changes their redox and electronic properties. Depending on the molecule geometry (linear or nonlinear), the number of nitrogen atoms and their distribution within the conjugated core, their ionization potential (IP) and electron affinity (EA) can be tuned in a wide range.[4] In addition to their interesting electronic properties, photo- and electroluminescence from acenes and azaacenes becomes possible. These properties make them suitable new candidates for use as electroluminophores. The potential importance of these new materials was highlighted last year by the decision of the United Nations proclaiming 2015 as the International Year of Light and Light based Technologies, with the principal goal of searching for new light sources free of toxic elements which, in addition, are less expensive in operation than current ones. In this respect organic materials can easily compete with inorganic counterparts, like for example nanocrystalline forms of inorganic semiconductors.[5]

Many acenes[6] and azaacenes[7] exhibiting high photo- and electroluminescence quantum yields (Q.Y.) have been reported as the active components of organic light emitting diodes (OLEDs).

In recent years, synthetic strategies leading to new organic semiconductors, in general, and to linear and nonlinear acenes and azaacenes in particular, frequently involved modification of old and sometimes almost forgotten dyes.[7d,e,8] In these cases the target azaacene core was first obtained in one step and then functionalized with solubilizing side groups such as triisopropylsilylethynyl ones forming a -C≡C- linkage with the core in a second step.[1] Other groups linking the solubilizing side chain with the core such as -CH_2-NH- or -CH=N- groups were also synthesised.[9] Recently, in the synthesis of several acenes, bistetracene diketone, first reported in 1949, was used as a substrate, to which two triisopropylsilylethynyl groups were attached, giving good solubility of the functionalized semiconductors in organic solvents.[10]

Several substrates known from the synthesis of dyes can also be exploited in the preparation of azaacenes. These are, among others, derivatives of aminoanthraquinone or diketopyrrolopyrrole. The synthetic pathway usually involves

[a] K. Kotwica, Dr. P. Bujak,* W. Krzywiec, D. Wamil, Dr. P. A. Gunka, L. Skorka, Prof. A. Pron,
Faculty of Chemistry, Warsaw University of Technology
Noakowskiego 3, 00-664 Warsaw, Poland.
E-mail: piotrbujakchem@poczta.onet.pl
[b] Dr. P. Data, Prof. A. P. Monkman,*
Durham University, Physics Department, South Road, DH1 3LE, UK. E-mail: a.p.monkman@durham.ac.uk
[c] Dr. P. Data,
Faculty of Chemistry, Silesian University of Technology, M. Strzody 9, 44-100 Gliwice, Poland.
[d] T. Jaroch, Prof. R. Nowakowski.
Institute of Physical Chemistry, Polish Academy of Science, Kasprzaka 44/52, 01-224 Warsaw, Poland.

Supporting information for this article is given via a link at the end of the document.

simple condensation reactions or oxidative C-N coupling, eliminating in this manner expensive palladium-based catalytic systems.[11]

At the beginning of 20th century, extensive research was carried out aimed at the search and development of new dyes which gave as one product a new, blue color vat dye, 6,15-dihydrodinaptho[2,3-*a*:2',3'-*h*]phenazine-5,9,14,18-tetraone, commonly termed indanthrone which was synthesized through condensation of aminoanthraquinone carried out at temperatures below 270 °C in basic conditions. At temperatures above 270 °C benzo[*h*]benz[5,6]acridino[2,1,9,8-*klmna*]acridine-8,16-dione (flavanthrone), a yellow vat dye, could be obtained from the same substrate (see ***Scheme 1***).

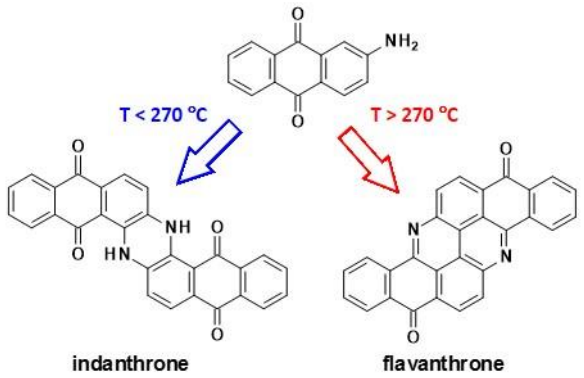

Scheme 1. Indanthrone (6,15-dihydrodinaptho[2,3-*a*:2',3'-*h*]phenazine-5,9,14,18-tetraone) and flavanthrone (benzo[*h*]benz[5,6]acridino[2,1,9,8-*klmna*]acridine-8,16-dione) from aminoanthraquinone.

In our previous papers we concentrated on indanthrone transforming it into a solution processable organic semiconducting derivative, namely 5,9,14,18-tetraalkoxy-dinaphtho[2,3-*a*:2',3'-*h*]phenazines in a simple one-pot process consisting of the reduction of the carbonyl group by sodium dithionite followed by substitution with solubility inducing groups under phase transfer catalysis conditions.[7d,e] The resulting compounds showed high photoluminescence quantum yield values and could be applied as electroluminophores in guest/host-type light emitting diodes. In this paper we present a systematic study on the synthesis, spectroscopic, structural (including self-assembly) and electrochemical properties of new solution processable, electroactive, conjugated molecules derived from flavanthrone showing that in many respects they are distinctly different from the indanthrone derivatives. We also describe guest/host light emitting diodes in which these new electroactive materials are used as electroluminophores.

Results and Discussion

The synthesis of flavanthrone has been known for over 100 years,[12] however, it has had to be modified to meet the standards of modern organic chemistry and to improve the reaction yield. Flavanthrone is also commercially available, but requires additional purification when used for the preparation of new semiconductors.

Flavanthrone (benzo[*h*]benz[5,6]acridino[2,1,9,8-*klmna*]acridine-8,16-dione) (see ***Scheme 2***) was obtained from 2-aminoanthraquinone **(1),** which in the first step was converted into its monobromo derivative **(2)** through the reaction with *N*-bromosuccinimide (NBS) in the 1:1 molar ratio. In the second step, the amine group was protected to yield **(3)**. Then an Ullmann C-C coupling reaction was carried out with high yield (95%).[13] In the last step a spontaneous reaction of the carbonyls with the amine groups took place upon deprotection, to yield the fused structure of flavanthrone **(5)**.

Flavanthrone was converted into 8,16-dialkoxy-benzo[*h*]benz[5,6]acridino[2,1,9,8-*klmna*]acridine in a one-pot process, previously elaborated for indanthrone.[7d] In the first step the carbonyl groups were reduced to phenolates using $Na_2S_2O_4$ in sodium hydroxide solution, then, without the necessity of intermediate product isolation, O-alkylation of phenolate groups was performed using alkyl bromides. It should be pointed out that the application of $Na_2S_2O_4$ as a reducing agents also has a long history since this reagent was used in coloring fabrics in old procedures employing vat dyes. The reaction pathway is presented in **scheme 2** and the exact preparation procedures can be found *Supporting Information*. Five derivatives with increasing alkoxy chain length were synthesized: -O-C_4H_9 (**FC-4**), -O-C_6H_{13} (**FC-6**), -O-C_8H_{17} (**FC-8**), -O-$C_{10}H_{21}$ (**FC-10**) and -O-$C_{12}H_{25}$ (**FC-12**)

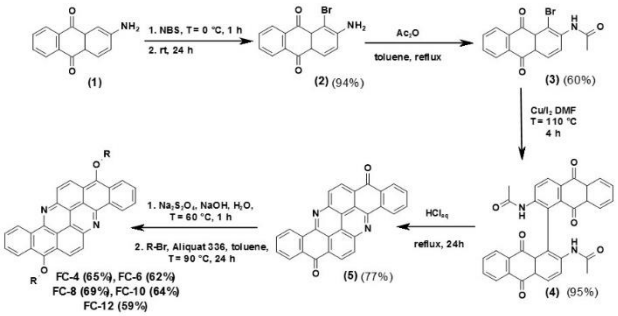

Scheme 2. Synthetic route to dialkoxy-derivatives of benzo[*h*]benz[5,6]acridino[2,1,9,8-*klmna*]acridine-8,16-dione (**FC-4-12**)

The ^{1}H NMR spectrum of **FC-8** is presented in **Figure 1a**. Since the molecule is symmetric, in the aliphatic part of the spectrum, at 4.43 ppm, only one triplet (J = 6.6 Hz) is observed corresponding to two equivalent -O-CH_2- groups in the alkoxy substituents. In the aromatic part of the spectrum (**Figure 1b**) five signals are observed, although six nonequivalent aromatic

protons can be distinguished in the molecule core. This implies that the spectral lines of two nonequivalent protons must overlap. Spectral lines corresponding to six nonequivalent aromatic protons are, however, clearly resolved in the case of **FC-6** (**Figure 1c**), which greatly facilitates unequivocal attribution of lines, especially as it is supported by the corresponding 1H-1H COSY spectrum (**Figure 1d**). Two well-resolved doublets at 8.44 and 8.63 ppm (J = 9.7 Hz) correspond to H(A) and H(B) of the diazapyrene core. The doublet at 10.30 ppm (J = 8.2 Hz) is attributed to the highly deshielded H(C) proton located in the vicinity of the hexyloxy substituent whereas the doublet at 8.77 ppm (J = 8.2 Hz) is ascribed to the H(F) proton. These two doublets, despite having the same value of the coupling constant, do not originate from the coupling of H(C) and H(F) protons as clearly concluded from the COSY spectrum. The observed chemical shifts of aromatic protons are in very good accordance with the literature data reported for benzo[*h*]benz[5,6]acridino[2,1,9,8-*klmna*]acridine-8,16-dione containing triisopropylsilylethynyl solubilizing substituents.[8b]

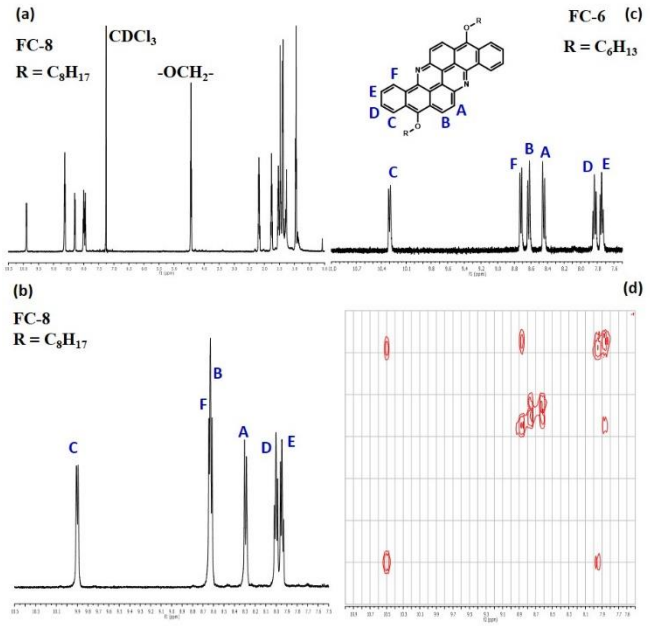

Figure 1. ^{1}H NMR spectra of: a) **FC-8** (whole range); b) **FC-8** (aromatic part); c) **FC-6** (aromatic part); d) **FC-6** 1H-1H COSY.

Redox properties of the synthesized molecules were studied by cyclic voltammetry. The voltammograms were measured from 5.0×10^{-4} M solutions of a given compound in 0.1 M Bu_4NBF_4/CH_2Cl_2 electrolyte and were essentially independent of the alkoxy substituent length. **Figure 2** shows a representative voltammogram for **FC-8.** As reported for alkoxy-substituted dinaphthophenazines (indanthrone derivatives) reported in [**7e**], **FC-8** undergoes an irreversible oxidation at positive potentials (*vs* Ag/0.1M Ag^+). However its electrochemical behavior at negative potentials is distinctly different since a *quasi*-reversible redox couple is found for this compound whereas the reduction of the previously studied alkoxy-substituted dinaphthophenazines is irreversible.

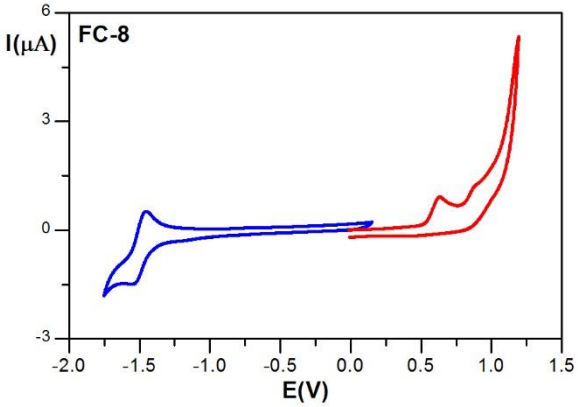

Figure 2. Cyclic voltammograms of **FC-8**, electrolyte 0.1 M Bu_4NBF_4 in CH_2Cl_2, scan rate = 50 mV/s, potential vs Ag/0.1M Ag^+.

From the onsets of the oxidation and reduction peaks potentials (+0.41 V and -1.62 V *vs* Fc/Fc^+, respectively) the ionization potential (IP) and the electron affinity (EA) can be calculated, using the following equations (**1**) and (**2**),[14] the results are listed in **Table 1**.

$$IP(eV) = |e|(E_{ox(onset)} + 4.8)(\mathbf{1})$$

$$EA(eV) = -|e|(E_{red(onset)} + 4.8)(\mathbf{2})$$

According to the literature data, the flavanthrone (*Vat Yellow 1*) shows IP = 6.3 eV and |EA| = 3.6 eV.[15] The value of IP obtained for **FC-8** (5.21 eV) is lower than that determined for tetraoctyloxy derivative of dinaphthophenazine (5.34 eV)[7e] whereas |EA| is higher (3.18 eV and 2.94 eV, respectively). This differences can be considered as a manifestation of a better conjugation within the more fused 4,9-diazapyrene ring as compared to phenazine one, which facilitates donor-acceptor interactions between the substituent and the *N*-substituted rings. It is also interesting to compare the IP value of **FC-8** with IP determined electrochemically for a molecule of the same core but different solubilizing substituents, namely triisopropylsilylethynyl groups, reported in ref. [**8b**]. The latter shows higher IP (5.36 eV) as compared to the case of **FC-8**, again in accordance with stronger electron donating properties of the alkoxy group facilitating the oxidation of **FC-8.** No electrochemical data for the reduction process of this triisopropylsilylethynyl derivative can be found in ref [**8b**].

Table 1 HOMO and LUMO levels of **FC-8** derivative along with corresponding Eg and ionization potential and electron affinity calculated at B3LYP/6-31G(d,p) level of theory. IP and |EA| values determined from cyclic voltammetry (CV) are shown for comparison

HOMO (A_u) (vacuum) (eV)	LUMO (A_g) (vacuum) (eV)	HOMO (A_u) (CH_2Cl_2) (eV)	HOMO (A_u) (CH_2Cl_2) (eV))	IP (DFT, CH_2Cl_2) (eV)	|EA| (DFT, CH_2Cl_2) (eV)	IP (CV, CH_2Cl_2) (eV)	|EA| (CV, CH_2Cl_2) (eV)
-4.95	**-2.42**	**5.13**	**2.61**	**5.03**	**2.70**	**5.21**	**3.18**

In polyconjugated systems the first oxidation process leads to the formation of a radical cation whereas the first reduction process to a radical anion. It is therefore helpful to analyze these redox processes in connection to the plots of frontier orbitals and spin density distribution of the radical ions formed. These plots are presented in **Figure 3**.

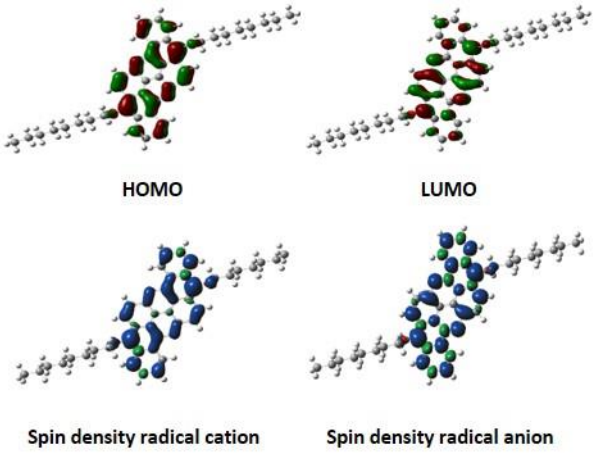

Figure 3. Frontier molecular orbital plots for **FC-8** (up, isosurface value = 0.03) and spin densities for radical cation and anion forms of this compound (down, isosurface value = 0.001).

Both HOMO and LUMO occupy the central fused aromatic core of the molecule, that is the HOMO is located mainly on the edge of this skeleton with the highest contribution from the carbon atom attached to the oxygen atom of the alkoxy substituent and with zero contribution from the two central carbon atoms. The LUMO on the other hand is more "pushed" towards the central part of the molecule also experiencing a strong contribution from the aforementioned C-O carbon and from the nitrogen atoms. When moving to spin density distribution in radical ions one can notice a similar behavior. The radical cation spin density is mainly located in the proximity of C-O carbon, with no contribution from the central part of the ring, while in the case of the radical anion it additionally occupies the space near the nitrogen atoms.

The DFT calculations also enable the determination of the IP and EA values of isolated molecules and molecules in a given solution, in the latter case using the polarizable continuum model (PCM). IP and EA values of **FC-8** were calculated for dichloromethane solutions *i.e*. the same solvent which was used in the cyclic voltammetry determination of the same parameter. The results are collected in **Table 1**. Better agreement between the theoretical and experimental values was obtained for IP, EA values differed by 0.48 eV. However, when compared to the indanthrone case, one sees that the overall match between the theory and the experiment is far better.

Solution absorption and emission spectra of the various derivatives are essentially independent of the length of the alkoxy substituent. In **Figure 4** the spectrum of **FC-8** dissolved is shown as a representative example, whereas the spectra of other derivatives are collected in *Supporting Information*.

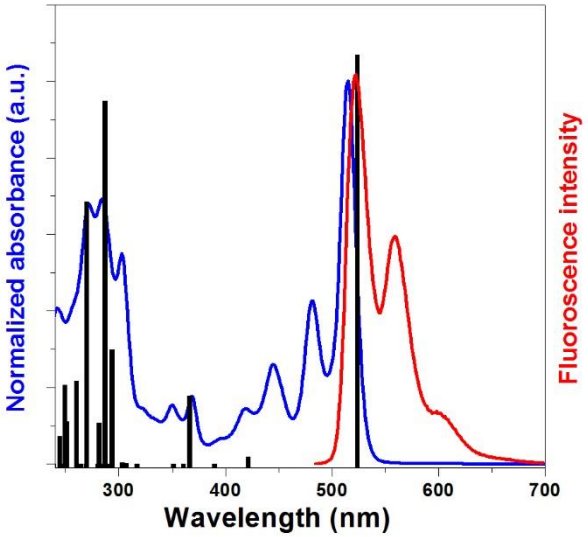

Figure 4. Absorption and emission spectra of **FC-8** (chloroform as a solvent). The calculated positions and relative oscillator strengths of the electronic transitions of this compound, obtained from TD DFT calculations, are depicted as black bars for comparison.

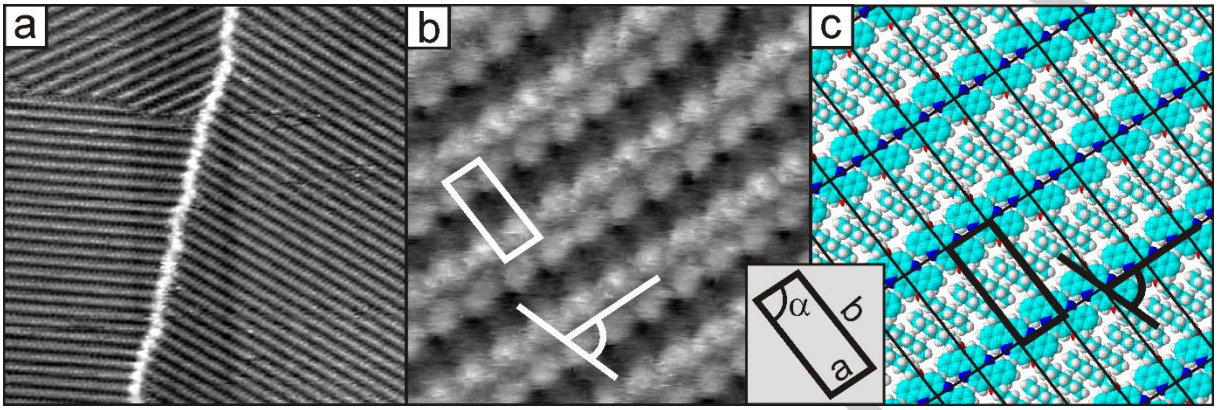

Figure 5. (**a,b**) STM images and (**c**) proposed adsorption geometry of a monolayer of **FC-8** on HOPG. Scanning area and parameters: (**a**) 61 x 61 nm^2, (**b**) 9 x 9 nm^2, V_{bias} = 1 V, I_t = 0.3 nA.

Features typical of periacenes and periazaacenes can be found in these spectra.[8b,10,16] These compounds usually show a set of absorption bands originating from $\pi \rightarrow \pi^*$ and $n \rightarrow \pi^*$ transitions which are being bathochromically shifted with increasing size of the aromatic core.[4c,17] Pronounced vibronic character of the lowest energy band (at 515 nm for *0-0* transition) should be pointed out. The spectrum is consistent with the calculated transistions (see **Figure 4** and **Table S2** in *Supporting Information*). The strongest band at 515 nm is almost purely H→L in nature (98%). This transistion is favored in centrosymetric (C_i point group) molecules such as **FC-8**, since the frontier orbitals (HOMO and LUMO) by symmetry belong to two different irreducible representations, A_u and A_g, respectively, the H→L transition is highly allowed according to the Laporte selection rule. Full analysis of the electronic transition can be found in *Supporting Information*.

The optical band gap of **FC-8**, $E_{gopt.}$, determined from the onset of the lowest energy absorptiion band, is 2.33 eV *i.e.* 100 meV larger than the gap in isopropylsilylethynyl functionalized periazaacene of the same core.[8b] It is however 70 meV smaller than the band gap of 5,9,14,18-tetraoctyloxydinaphtho[2,3-*a*:2',3'-*h*]phenazine (the corresponding indanthrone derivative).[7e]

All compounds of the **FC-n** series exhibit strong green photoluminescence. Their emission spectra can be treated as mirror images of the absorption ones (see **Figure 4** where the emission and absorption spectra of **FC-8** are shown as an example). This feature, together with a very small Stokes shift of 9 nm clearly indicate a very similar molecule geometry in the ground and excited states consistent with the rigid nature of the core. It is also worth noting that the experimental emission wavelength corresponds very well with the one calculated *via* state-specific TD-DFT where the theoretical λ_{em} is 554 nm. The measured photoluminescence quantum yield (PLQY) in all cases reaches 80%, a value which is significantly higher than that measured for tetraalkoxydinaphthophenazines, the corresponding indanthrone derivatives (*ca.* 60%).[7e]

As with tetraalkoxydinaphthophenazines[8b], compounds of the **FC-n** series are capable of self-assembling into highly ordered 2D supramolecular structures in monolayers deposited on suitable substrates such as HOPG, for example. **Figure 5a,b** shows representative STM images of a monolayer of **FC-8** deposited on a HOPG substrate. The adsorbate molecules are well-organized into large domains of typical size of a few hundred nanometers which differ in their orientation (see upper part of the large-scale image in **Figure 5a**). Each domain is observed by STM as a set of parallel bright stripes corresponding to rows of molecules oriented in one direction.

Images obtained at higher magnification (**Figure 5b**) provide more detailed information concerning the arrangement of individual molecules in the monolayer. Each stripe, clearly visible in this image, is characterized by its inner structure which consists of two rows of well resolved bright spots. It is expected that this signal of higher tunneling current corresponds to the conjugated cores of the investigated adsorbate. Microscopic investigations performed with different bias potentials (not discussed in this paper) enabled us to postulate the orientation of molecules in the observed rows. This direction (70º with respect to the direction of the row orientation) is marked schematically in **Figure 5b** by an angle indicated in white. Each molecule is therefore visible at submolecular resolution as a set of two bright spots oriented along this axis. The 2D unit cell parameters determined from the STM images are: 0.91 ± 0.05 nm / 2.30 ± 0.1 nm /84º ±2°. The corresponding model of adsorption geometry is presented in **Figure 5c**. The dimension of the unit cell along its shorter axis (0.91 nm) indicates that the fused aromatic cores of adjacent molecules are tightly packed in this direction. This correlation also shows that in the monolayer the conjugated cores of the molecules lie flat on the substrate surface. The

molecular rows formed in this way are separated by a distance of 2.30 nm imposed by the interdigitation of alkyl substituents.

We further investigated the self-organization 2D pattern to determine how the observed monolayer structure of **FC-8** is related to its 3D organization in a single crystal. Crystal structure analysis revealed that **FC-8** crystallizes in the $P\bar{1}$ triclinic space group. The molecule consists of a flat aromatic core and two *n*-octyloxy groups in the *anti* conformation (see **Figure 6** for the molecular structure of **FC-8**). The root mean square displacement of atoms constituting the aromatic core from the mean plane equals 0.052 Å whereas the C29−O1−O2−C37 torsion angle describing the mutual orientation of alkoxy groups amounts to 178.8(3)°. Inversion-related molecules form dimers *via* π-stacking accompanied by C−H···O interactions (**Figure 7**, *d*(C29···O2^{i}) = 3.332(4) Å, *d*(H29B···O2^{i}) = 2.44 Å C29−H29B···O2 = 150°, i = 1 – *x*, 1 – *y*, 1 – *z*). The dimers in turn form π-stacked columns running along [100] direction (**Figure S2** in *Supporting Information*). The distance between mean planes of the aromatic cores in the dimers is 3.4398(11) Å with the plane shift of 1.7825(12) Å while the interplanar distance between molecules from the adjacent dimers equals 3.3030(15) Å but the plane shift is 7.8503(14) Å (**Figure S2** in *Supporting Information*). Columns are held together in the 3D structure by dispersion forces mainly between interdigitated alkyl chains. In this crystalline arrangement it is possible to identify an almost flat and densely packed slices of molecules whose 2D ordering is very similar to that found in the monolayer deposited on HOPG (**Figure S3** in *Supporting Information*). The 2D unit cell parameters of the slice are 0.9365(4) nm/2.3929(4) nm/86.86(2)° confirming the unit cell parameters of the monolayer determined from STM measurements (corresponding parameters 0.91 ± 0.05 nm / 2.30 ± 0.1 nm /84º ± 2º).

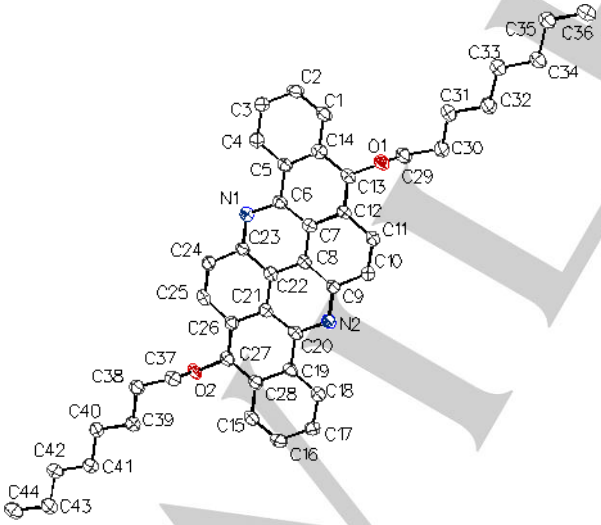

Figure 6. Molecular structure of **FC-8** with atom numbering scheme. Thermal ellipsoids drawn at 50% probability level and hydrogen atoms omitted for clarity.

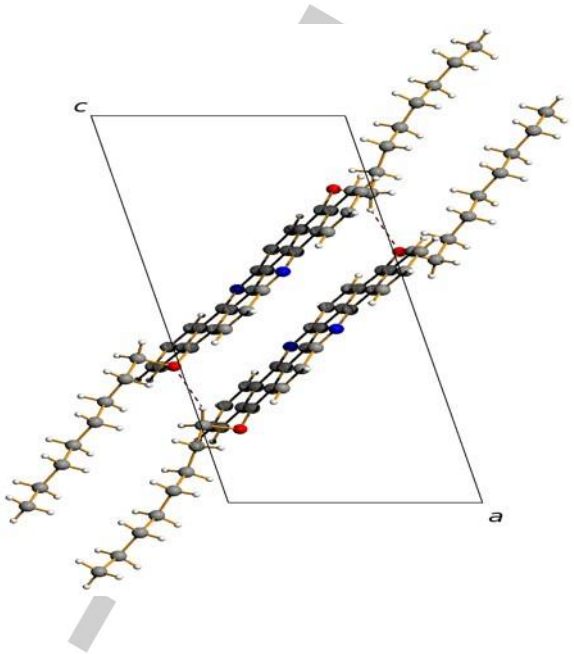

Figure 7. Unit cell of **FC-8** crystal structure viewed along [010] direction. C−H···O hydrogen bonds drawn as dashed brown lines. Ball-and-stick model used.

Triisopropylsilylethynyl-substituted analogue of the **FC-n** series of compounds also readily forms single crystals and for this reason it was used in the fabrication of single crystals field effect transistors (FETs) showing reasonable hole mobility.[8b] Taking into account the excellent luminescent properties of all **FC-n** derivatives (PLQY of 80%) we explored their application as high mobility electroluminophores in OLEDs, especially in view of the fact that such applications of are extremely rare in the case of azaacenes and periazaacenes.[7d-f,18]

The device structure used for guest/host-type diodes was; ITO/PEDOT:PSS/PVK/(**FC**-(**4**,**8**,**12**)-CBP/TPBi/LiF/Al. The corresponding energy level scheme for this structure is shown in **Figure 8a**. The emissive layer was varied for a range of emitter concentrations of 1% to 15% of a given **FC-n** compound molecularly dispersed in a 4,4'-bis(*N*-carbazolyl)-1,1'-biphenyl (CBP) matrix. This emissive layer is sandwiched between a hole transporting layer of poly(9-vinylcarbazole) (PVK) and a hole blocking layer of 2,2',2"-(1,3,5-benzinetriyl)-tris(1-phenyl-1-H-benzimidazole) (TPBi), in a hybrid solution co-vacuum deposition method. These two layers are separated from electrodes (ITO, and Al) by layers of PEDOT and LiF, respectively.

Table 2. Electroluminescence data for diodes containing **FC-4**, **FC-8** and **FC-12** (1-15 wt %) as electroluminophores.

	FC-4		FC-8		FC-12	
	(cd/m^2)[a]	(cd/A)[b]	(cd/m^2)	(cd/A)	(cd/m^2)	(cd/A)
1 wt %	1885	2.74	1860	3.06	1460	2.13
3 wt %	988	1.21	1790	1.17	1580	1.63
5 wt %	1100	0.96	717	0.34	262	0.12
10 wt %	746	0.66	619	0.39	54	0.23
15 wt %	500	0.29	-	-	155	0.16

a – luminance, b – luminous efficiency.

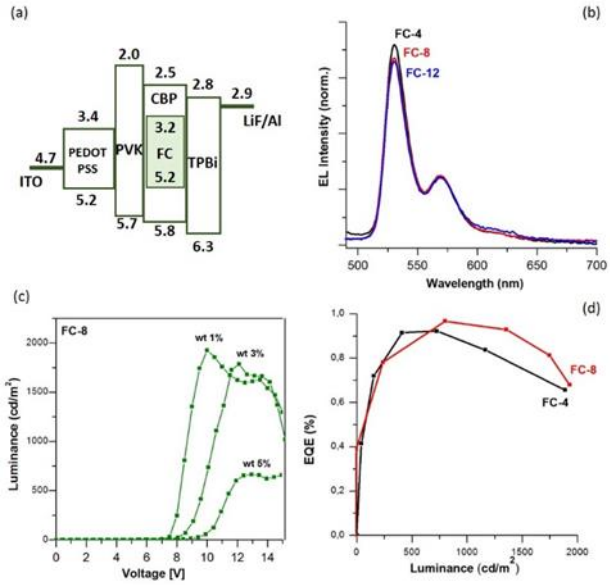

Figure 8. (**a**) Device structure and energy diagram of the green light emitting diode, (**b**) electroluminescence spectra of: 1 wt% dispersion of **FC-4** (black), **FC-8** (red) and **FC-12** (blue) in CPB matrix, (**c**) luminance *vs* voltage characteristics for diodes with active layers containing increasing amounts of **FC-8**: 1%, 3%, 5%, (**d**) external quantum efficiency *vs* luminance characteristics for OLEDs with **FC-4** and **FC-8** (1 wt%).

Figure 8b shows the electroluminescence spectrum measured for the emissive layer containing 1 % of the **FC-n** luminophore. These spectra resemble the photoluminescence spectra recorded from chloroform solutions of the studied luminophores with the vibrational structure retained, the emission peaks however being bathochromically shifted by 10 to 15 nm (compare **Figures 4** and **8b**). In **Figure 8c** plots of luminance *vs* voltage are shown for increasing contents of **FC-8** luminophore in the CBP matrix. It is clear that with increasing content of the electroluminophore the luminance decreases with simultaneous increase of the *turn on* voltage. This effect may suggest nanoaggregation occurring at higher electroluminophore contents which favours nonradiative quenching of the emitter. The parameters of all studied diodes are collected in **Table 2**. The highest luminance values (approaching 1900 cd/m^2) were obtained for **FC-4** and **FC-8** whereas the highest luminous efficiency (exceeding 3 cd/A) was found for **FC-8**. In the case of **FC-4** and **FC-8** the highest external quantum efficiencies (EQEs), exceeding 0.9%, were measured for moderate luminances but they never dropped below 0.65% for the whole range of luminances studied (see **Figure 8d**).

Conclusions

To summarize, we have demonstrated that by simple modification of benzo[*h*]benz[5,6]acridino[2,1,9,8-*klmna*]acridine-8,16-dione (flavanthrone), an old, intractable and almost forgotten vat dye, *via* reduction of its carbonyl groups to phenolates followed by their O-alkylation, it is possible to obtain a new group of solution processable, electroactive, conjugated molecules, namely 8,16-dialkoxy-benzo[*h*]benz[5,6]acridino[2,1,9,8-*klmna*]acridines. HOMO and LUMO energies of these compounds as well as their ionization potential (IP) and electron affinity (EA) values make these new compounds suitable candidates for the application as components of organic field effect transistors and light emitting diodes. This last possibility was explored and green emitting diodes were obtained in the guest/host configuration (with 4,4'-bis(*N*-carbazolyl)-1,1'-biphenyl (CBP) host). Self-assembly properties of these compounds should also be pointed out since they form monolayers at the surface of HOPG, in which highly ordered 2D supramolecular organization is extended over few hundreds of nanometers.

Experimental Section

Synthesis: The list of all chemicals together with detailed description of the synthesis of all investigated derivatives and the spectroscopic characterization data can be found in *Supporting Information*.

Spectroscopic Studies: ^{1}H NMR and ^{13}C NMR spectra were recorded on a Varian Unity Inova 500 MHz spectrometer and referenced with respect to TMS and solvents. The elemental analyses were carried out on a Vario EL III (Elementar) CHN analyzer. HRMS spectra were recorded in methanol on Mariner ESI-TOF (Applied Biosystems) mass spectrometer. Solution UV-vis-NIR spectra were recorded in chloroform on a Cary 5000 (Varian) spectrometer whereas the emission spectra were measured using an Edinburgh FS 900 CDT fluorometer (Edinburgh Analytical Instruments). Photoluminescence quantum yields were determined using quinine sulfate in 0.05 mol dm^{-3} H_2SO_4 (φ_{fl} = 0.51) as a standard.[19]

Cyclic Voltammetry: Cyclic voltammetry studies were performed in a three-electrode, one-compartment cell with a platinum working electrode (3 mm^2), a platinum wire counter electrode and a Ag/0.1 M $AgNO_3/CH_3CN$ reference electrode. A given flavanthrone derivative was dissolved in 0.1 M Bu_4NBF_4 in dichloromethane to yield 5×10^{-4} M solution.

Computational Methods: DFT calculations were carried out using Gaussian09 Revision D.01[20] package and employing hybrid B3LYP[21] exchange correlation potential combined with 6-31G(d,p) basis set. Ground- and excited-state geometries were fully optimized until a stable local minimum was found, which was confirmed by normal-mode analysis (no imaginary frequencies were present). Initial structures were constrained to the C_i symmetry point group and then relaxed if a saddle point was found. Solvent-solute interactions were taken into account with the aid of polarizable continuum model (PCM)[22] and dichloromethane as a solvent. The oscillator strengths and energies of the vertical singlet excitations were calculated employing time-dependant version (TD) of DFT[23] at respective optimized geometries. Multiconfigurational character of the most pronounced excitations was analyzed with Natural Transition Orbitals (NTO).[24] Excited-to-ground-state transitions were calculated *via* state-specific solvation approach taking into account the Franck-Condon rule.[25] The necessary data of DFT calculations was retrieved from output files using GaussSum 2.2.[26] All necessary initial geometries and final graphics (molecular orbitals and spin densities) were generated in GaussView 5.0.[27]

Scanning Tunneling Microscopy (STM): Monomolecular layers were prepared by drop-casting from a solution of the investigated compound in hexane (~2mg/L) on a freshly cleaved surface of highly oriented pyrolitic graphite (HOPG, SPI Supplies, USA). The layers dried under ambient conditions were then imaged in air at room temperature by means of an STM system (University of Bonn, Germany).[28] All images were recorded in a constant current mode using mechanically cut Pt/Ir (80/20 %) tips. The proposed real-space models of the monomolecular layers were obtained by the correlation of the layer structure deduced from the STM images and the molecular model of the investigated adsorbate determined using HyperChem software package.

X-ray Diffraction: Suitable single crystal of **FC-8** grown from chlorobenzene was selected under a polarizing microscope, mounted in inert oil (Paratone N) and transferred to the cold gas stream of the diffractometer. Diffraction data were collected on an Oxford Diffraction κ-CCD Gemini A Ultra diffractometer at 120(2) K with mirror-focused Cu-Kα radiation. Cell refinement and data collection as well as data reduction and analysis were performed with the CrysAlis^{PRO} software.[29] The structures were solved by direct methods and subsequent Fourier-difference synthesis with SHELXT and refined by full-matrix least-squares against F^2 with SHELXL-2014 within the Olex2 program suite.[30] All non-hydrogen atoms were refined anisotropically. Hydrogen atoms were introduced at calculated positions and refined as riding atoms. Data were analyzed using Olex2, Platon and Diamond.[30c,31] Crystal data and structure refinement parameters are given in **Table S3**. Images were created using Olex2 and Diamond and were rendered with POV-Ray.[30c,31b,32]

Electroluminescence Measurements and Light-Emitting Diode Fabrication: Guest-host type electroluminescent diodes were fabricated by molecular dispersion of either **FC-4** or **FC-8** or **FC-12** (1 to 15 wt %) in an one-component matrix consisting of 4,4'-bis(N-carbazolyl)-1,1'-biphenyl (CBP). Poly(9-vinylcarbazole) (PVK) and 2,2',2''-(1,3,5-benzinetriyl)-tris(1-phenyl-1-H-benzimidazole) (TPBi) were used as hole-transportin layer and hole-blocking layers, respectively. The active layer of ca. 50 nm was deposited on top of an ITO electrode precoated with a PEDOT:PSS layer of *ca.* 50 nm thickness and with a PVK layer of *ca.* 10 nm thickness. In the subsequent step a TPBi (50 nm) layer and an ultrathin (1 nm) LiF layer were evaporated followed by deposition of an Al layer. The fabricated devices were tested under ambient conditions. Characteristic of OLED devices were conducted in a 10 inch integrating sphere (Labsphere) connected to a Source Meter Unit (and calibrated with NIST calibration lamp)

Acknowledgements

This research was carried out in the framework of the project entitled "New solution processable organic and hybrid (organic/inorganic) functional materials for electronics, optoelectronics and spintronics" (Contract No. TEAM/2011-8/6), which is operated within the Foundation for the Polish Science Team Programme cofinanced by the EU European Regional Development Fund. K.K., P.B., L.S. and A. P. wish to acknowledge financial support from National Centre of Science in Poland (NCN, Grant No. 2015/17/B/ST5/00179). K.K., P.B., L.S. and A.P. wish to acknowledge financial support from National Centre of Science in Poland (NCN, Grant No. 2015/17/B/ST5/00179).

Keywords: flavanthrone • solution processable electroactive conjugated molecule • crystal structure • organic light emitting diodes • host/guest electroluminescent system

[1] a) J. E. Anthony, *Angew. Chem.* **2008**, *120*, 460-492; *Angew. Chem. Int. Ed.* **2008**, *47*, 452-483; b) U. H. F. Bunz, J. U. Engelhart, B. D. Lindner, M. Schaffroth, *Angew. Chem.* **2013**, *125*, 3898-3910; *Angew. Chem. Int. Ed.* **2013**, *52*, 3810-3821; c) C. Wang, P. Gu, B. Hu, Q. Zhang, *J. Mater. Chem. C* **2015**, *3*, 10055-10065; d) J. Li, Q. Zhang, *ACS Appl. Mater. Interfaces* **2015**, *7*, 28049-28062.

[2] a) V. C. Sundar, J. Zaumseil, V. Podzorov, E. Menard, R. L. Willett, T. Sorneya, M. E. Gershenson, J. A. Roger, *Science* **2004**, *303*, 1644-1646; b) H. Okamoto, N. Kwasaki, Y. Kaji, Y. Kubozono, A. Fujiwara, M. Yamaji, *J. Am. Chem. Soc.* **2008**, *130*, 10470-10471.

[3] J. E. Anthony, *Chem. Rev.* **2006**, *106*, 5028-5048.

[4] a) Z. Liang, Q. Tang, R. Mao, D. Liu, J. Xu, Q. Miao, *Adv. Mater.* **2011**, *23*, 5514-5518; b) Y. Sakamoto, T. Suzuki, M. Kobayashi, Y. Gao, Y. Fukai, Y. Inoue, F. Sato, S. Tokito, *J. Am. Chem. Soc.* **2004**, *126*, 8138-8140; c) Z. Liang, Q. Tang, J. Xu, Q. Miao, *Adv. Mater.* **2011**, *23*, 1535-1539; d) Q. Miao, *Adv. Mater.* **2014**, *26*, 5541-5549; e) C. Wang, J. Zhang, G. Long, N. Aratani, H. Yamada, Y. Zhao, Q. Zhang, *Angew. Chem.* **2015**, *127*, 6390-6394, *Angew. Chem. Int. Ed.* **2015**, *54*, 6292-6296.

[5] S. Reineke, *Nat. Mater.* **2015**, *14*, 459-462.

[6] a) J. Xiao, S. Liu, Y. Liu, L. Ji, X. Liu, H. Zhang, X. Sun, Q. Zhang, *Chem. Asian J.* **2012**, *7*, 561-564; b) Q. Zhang, Y. Divayana, J. Xiao, Z. Wang, E. R. T. Tiekink, H. M. Duong, H. Zhang, F. Boey, X. W. Sun, F. Wudl, *Chem. Eur. J.* **2010**, *16*, 7422-7426; c) J. Xiao, Y. Divayana, Q. Zhang, H. M. Duong, H. Zhang, F. Boey, X. W. Sun, F. Wudl, *J. Mater. Chem.* **2010**, *20*, 8167-8170.

[7] a) C. Fu, M. Li, Z. Su, Z. Hong, W. Li, B. Li, *Appl. Phys. Lett.* **2006**, *88*, 093507; b) X. Xu, G. Yu, S. Chen, C. Di, Y. Liu, *J. Mater. Chem.* **2008**, *18*, 299-305; c) K-i. Nakayama, Y. Hashimoto, H. Sasabe, Y.-J. Pu, M. Yokoyama, J. Kido, *Jpn, J. Appl. Phys.* **2010**, *49*, 01AB11; d) K. Kotwica, P. Bujak, D. Wamil, M. Materna, L. Skorka, P. A. Gunka, R. Nowakowski, B. Golec, B. Luszczynska, M. Zagorska, A. Pron, *Chem. Commun.* **2014**, *50*, 11543-11546; e) K. Kotwica, P. Bujak, D. Wamil, A. Pieczonka, G. Wiosna-Salyga, P. A. Gunka, T. Jaroch, R. Nowakowski, B. Luszczynska, E. Witkowska, I. Glowacki, J. Ulanski, M. Zagorska, A. Pron, *J. Phys. Chem. C* **2015**, *119*, 10700-10708; f) P.-Y. Gu, Y. Zhao, J.-H. He, J. Zhang, C. Wang, Q.-F. Xu, J.-M. Lu, X. W. Sun, Q. Zhang, *J. Org. Chem.* **2015**, *80*, 3030-3035.

[8] a) L. Zhang, B. Walker, F. Liu, N. S. Colella, S. C. B. Mannsfeld, J. J. Watkins, T.-Q. Nguyen, A. L. Briseno, *J. Mater. Chem.* **2012**, *22*, 4266-4268; b) L. Zhang, A. Fonari, Y. Zhang, G. Zhao, V. Coropceanu, W. Hu, S. Parkin, J.-L. Brédas, A. L. Briseno, *Chem. Eur. J.* **2013**, *19*, 17907-17916; c) M. K. Węcławski, M. Tasior, T. Hammann, P. J. Cywiński, D. T. Gryko, *Chem. Commun.* **2014**, *50*, 9105-9108.

[9] J.-B. Giguère, J.-F. Morin, *J. Org. Chem.* **2013**, *78*, 12769-12778.

[10] L. Zhang, A. Fonari, Y. Liu, A.-L. M. Hoyt, H. Lee, D. Granger, S. Parkin, T. P. Russell, J. E. Anthony, J.-L. Brédas, V. Coropceanu, A. L. Briseno, *J. Am. Chem. Soc.* **2014**, *136*, 9248-9251.

[11] a) K. Goto, R. Yamaguchi, S. Hirato, H. Ueno, T. Kawai, H. Shinokubo, *Angew Chem.* **2012**, *124*, 10479-10482; *Angew. Chem. Int. Ed.* **2012**, *51*, 10333-10336; b) W. Yue, S.-L. Suraru, D. Bialas, M. Müller, F. Würthner, *Angew. Chem.* **2014**, *126*, 6273-6276; *Angew. Chem. Int. Ed.* **2014**, *53*, 6159-6162; c) D. Sakamaki, D. Kumano, E. Yashima, S. Seki, *Angew. Chem.* **2015**, *127*, 5494-5497; *Angew. Chem. Int. Ed.* **2015**, *54*, 5404-5407.

[12] R. Scholl, H. Berblinger, *Chem. Ber.* **1903**, 36, 3427-3445.

[13] a) A. Schuhmacher, *Deutche Patent*, DPMA DE1955157; b) B. Rastoin, *Deutche Patent*, DPMA DE1944276.

[14] a) S. Trasatti, *Pure Appl. Chem.* **1986**, *58*, 955-966; b) C. M. Cardona, W. Li, A. E. Kaifer, D. Stockdale, G. C. Bazan, *Adv. Mater.* **2011**, *23*, 2367-2371; c) R. Rybakiewicz, P. Gawrys, D. Tsikritzis, K. Emmanouil, S. Kennou, M. Zagorska, A. Pron, *Electrochim. Acta* **2013**, *96*, 13-17.

[15] E. D. Głowacki, L. Leonat, G. Voss, M. Bodea, Z. Bozkurt, M. Irima-Vladu, S. Bauer, N. S. Sariciftci, *Proc. SPIE* **2011**, *8118*, 81180M.

[16] E. Ahmed, A. L. Briseno, Y. Xia, S. A. Jenekhe, *J. Am. Chem. Soc.* **2008**, *130*, 1118-1119.

[17] S. Miao, A. L. Appleton, N. Berger, S. Barlow, S. R. Marder, K. I. Hardcastle, U. H. F. Bunz, *Chem. Eur. J.* **2009**, *15*, 4990-4993.

[18] B. D. Lindner, Y. Zhang, S. Höfle, N. Berger, C. Teusch, M. Jesper, K. I. Harcastle, X. Qian, U. Lemmer, A. Colsmann, U. H. F. Bunz, M. Hamburger, *J. Mater. Chem. C* **2013**, *1*, 5718-5724.

[19] R. A. Velapoldi, Proceedings on the 1972 Conference on Accuracy in Spectrophotometry and Luminescence Measurements, National Bureau of Standards Special Publ. 378; U.S. Govt. Print Office, Washington, DC, 1973; p 231.

[20] M. J. Frisch, G. W. Trucks, H. B. Schlegel, G. E. Scuseria, M. A. Robb, J. R. Cheeseman, G. Scalmani, V. Barone, B. Mennucci, G. A. Petersson, *et al. Gaussian 09*, Revision D.01; Gaussian, Inc., Wallingford CT, 2013.

[21] a) A. D. Becke, *J. Chem. Phys.* **1993**, *98*, 1372-1377; b) A. D. Becke, *J. Chem. Phys.* **1993**, *98*, 5648-5652; c) C. T. Lee, W. T. Yang, R. G. Parr, *Phys. Rev. B* **1988**, *37*, 785-789.

[22] J. Tomasi, B. Mennucci, R. Cammi, *Chem. Rev.* **2005**, *105*, 2999-3093.

[23] a) R. Bauernschmitt, R. Ahlrichs, *Chem. Phys. Lett.* **1996**, *256*, 454-464; b) M. E. Casida, C. Jamorski, K. C. Casida, D. R. Salahub, *J. Chem. Phys.* **1998**, *108*, 4439-4449; c) R. E. Stratmann, G. E. Scuseria, M. J. Frisch, *J. Chem. Phys.* **1998**, *109*, 8218-8224; d) C. van Caillie, R. D. Amos, *Chem. Phys. Lett.* **1999**, *308*, 249-255; e) C. van Caillie, R. D. Amos, *Chem. Phys. Lett.* **2000**, *317*, 159-164; f) F. Furche, R. Ahlrichs, *J. Chem. Phys.* **2002**, *117*, 7433-7447; g) G. Scalmani, M. J. Frisch, B. Mennucci, J. Tomasi, R. Cammi, V. Barone, *J. Chem. Phys.* **2006**, *124*, 094107-1-094107-15.

[24] R. L. Martin, *J. Chem. Phys.* **2003**, *118*, 4775-4777.

[25] a) R. Improta, V. Barone, G. Scalmani, M. J. Frisch, *J. Chem. Phys.* **2006**, *125*, 054103-1-054103-9; b) R. Improta, G. Scalmani, M. J. Frisch, V. Barone, *J. Chem. Phys.* **2007**, *127*, 074504-1-074504-9.

[26] N. M. O'Boyle, A. L. Tenderholt, K. M. Langner, *J. Comput. Chem.* **2008**, *29*, 839 -845.

[27] R. Dennington, T. Keith, J. Millam, *GaussView*, Version 5, *Semichem Inc.,* Shawnee Mission, KS, 2009.

[28] M. Wilms, M. Kruft, G. Bermes, K. Wandelt, *Rev. Sci. Instrum.* **1999**, *70*, 3641-3650.

[29] *CrysAlisPro Software system ver. 171.37.35*, Agilent Technologies UK Ltd, Oxford, UK, 2014.

[30] a) G. M. Sheldrick, *Acta Crystallogr. A* **2015**, *71*, 3-8; b) G. M. Sheldrick, *Acta Crystallogr. C* **2015**, *71*, 3-8; c) O. V. Dolomanov, L. J. Bourhis, R. J. Gildea, J. A. K. Howard, H. Puschmann, *J. Appl. Crystallogr.* **2009**, *42*, 339-341.

[31] a) A. L. Spek, *J. Appl. Crystallogr.* **2003**, *36*, 7-13; b) *Diamond ver. 3.2k*, Crystal Impact GbR, Bonn, Germany, 2014.

[32] *Persistence of Vision (TM) Raytracer (POV-RAY)*, Persistence of Vision Pty. Ltd, Williamstown, Victoria, Australia, 2010.

Entry for the Table of Contents

Layout 1:

FULL PAPER

Soluble Flavanthrone Derivatives: Synthesis, Characterization and Application to Organic Light Emitting Diodes

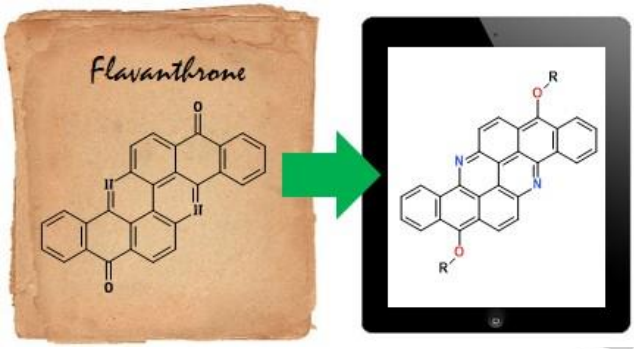

*Author(s), Corresponding Author(s)**

Page No. – Page No.

Title